THE TURBULENT/NON-TURBULENT INTERFACE OF A COOLED JET

J. Westerweel, A. Petracci, R. Delfos, J.C.R. Hunt
Laboratory for Aero & Hydrodynamics,
Delft University of Technology
Leeghwaterstraat 21, 2628 CA Delft, Netherlands
j.westerweel@tudelft.nl

ABSTRACT

The turbulent/non-turbulent interface of a jet is characterized by sharp jumps ('discontinuities') in the conditional flow statistics relative to the interface. Experiments were carried out to measure the conditional flow statistics for a cooled jet. These experiments are complementary to the experiments reported by Westerweel et al. (2005) on a Re=2000 jet, where the thermal diffusivity is intermediate the diffusivity of momentum and the diffusivity of mass. The experimental method is a combined LIF/PIV method, where a temperature-sensitive fluorescent dye (rhodamine 6G) is used to measure the instantaneous temperature fluctuations. The results show that the cooled jet can be considered to behave like a self-similar jet without any buoyance effects. The detection of the interface is based on the instantaneous turbulent kinetic energy, and provides a reliable means to detect the interface. Conditional flow statistics reveal the superlayer jump in the conditional vorticity and in the temperature.

INTRODUTION

Free turbulent flows, such as wakes, mixing layers, and jets, are bounded by regions of irrotational fluid. The interface between the turbulent and non-turbulent fluid is usually very sharp. The interface is continuously deformed by the turbulent flow, so it has a strongly contorted shape over a wide range of scales. The sharp interface is in strong contrast to the mean flow properties, which show a very gradual change from the turbulent to the non-turbulent flow region. This gradual change is the result of intermittency, in which turbulent and non-turbulent flow regions pass along a fixed point.

A long-standing problem about these unconfined, but localized, turbulent flows is to describe and quantify the characteristic features of the inhomogeneous interface (Hinze 1975; Townsend 1976; Hunt et al. 2001; Tsinober 2001), and to identify the nature of the entrainment process by which irrotational fluid becomes turbulent. Until recently it had been unclear whether this occurs as the result of outward spreading of small-scale vortices (nibbling) or large-scale engulfment by the inviscid action of the dominant eddies in the turbulent flow region. Results obtained from numerical simulations indicate that engulfment is not the dominant process (Mathew and Basu 2002), in contrast to conclusions from many earlier studies (Townsend 1976; Brown and Roshko 1974). Bisset et al. (2002) analyzed the flow properties in relation to the instantaneous position y_i of the interface. This showed that there is a jump in the conditional flow statistics at the interface. This jump is related to the laminar superlayer that was first described by Corrsin and Kistler (1955). Recent experimental findings (Westerweel et al. 2005) revealed the existence of a superlayer at the turbulent/non-turbulent interface of a submerged jet. The measurements also indicated that the motion at the interface is dominated by small scales, and that entrainment is predominantly a small-scale process (i.e., nibbling). Similar observations were done for the progressing turbulent/non-turbulent interface in a tank with an osillating grid (Holzner et al. 2006).

In this paper we present the continuation of the jet experiments. Rather than using a dye with a high Schmidt number (Sc$\sim$2300 for fluorescein dissolved in water), we use a slightly cooled jet to investigate the mechanics of the interface for a scalar with a higher diffusivity (the Prandtl number for water is about 10).

EXPERIMENTAL

The experimental configuration is almost identical to the one used by (Fukushima et al. 2002) for the measurement of the mixing of the turbulent jet fluid, marked by means of a fluorescent dye, with the ambient fluid. We now apply a temperature-sensitive fluorescent dye, i.e. rhodamine 6G, to both the jet fluid and the ambient fluid. The characteristics of this dye are described by Walker (1987). The fluorescence intensity of this dye is inversely proportional to the fluid temperature with a sensitivity of 1.8%/K. For the purpose of the PIV measurements the fluid has been seeded with small 8-12 μm diameter neutrally buoyant tracer particles.

The test section consists of a rectangular chamber of $110\times110\times300$ mm^3. The jet fluid flows through a small stainless steel tube with a 1 mm inner diameter into the test section. Glass windows on four sides of the test section allow for optical access for both the illumination light sheet and the LIF and PIV cameras.

The flow is illuminated with a thin light sheet (1 mm thickness) through the jet axis. The light sheet is generated from a double-cavity pulsed Nd:YAG laser with a maximum pulse energy of 200 mJ with a light wavelength of 532 nm and a maximum repetition rate of 15 Hz. (The actual repetition rate is lower and is determined by the framing rate of the cameras.) The rhodamine 6G absorbs (part of) the (green) illumination light, which is emitted at a longer wavelength around 590 nm (viz., red light). Two cameras are used to record the LIF signal (i.e., the light emitted by the fluorescent dye) and the PIV signal (i.e., the light scattered by the PIV tracer particles) separately. A diagram of the optical configuration is shown in Figure 1.

A beam splitter separates the light from the test section along two optical paths. The fluorescent light is separated from the light scattered by the tracer particles by means of a suitable optical band-pass filter that transmits the fluorescent light and blocks the (green) light scattered by the tracer particles. Along the other optical path a narrow-band interference filter only passes the monochromatic scattered light with a 532 nm wavelength from the tracer

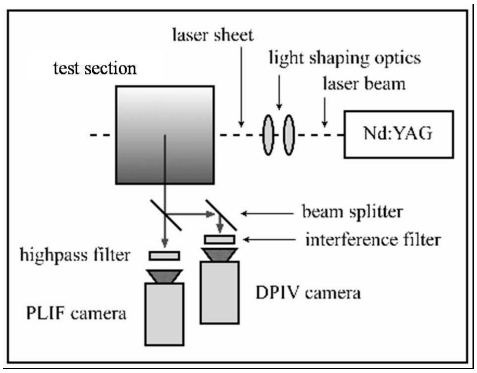

Figure 1: Schematic of the optical configuration for the combined LIF and PIV measurements.

particles. This configuration effectively separates the LIF and PIV signals without any unwanted cross talk.

In this experiment we use a single laser for both the LIF and PIV measurements. It is more common to use two different lasers for combined LIF and PIV, as the LIF generally requires a laser source with a good beam quality, whereas the PIV requires a high-energy pulsed laser (Hishida and Sakakibara 2000). Pulsed lasers generally have poor beam quality and the total energy can vary substantially between subsequent pulses. The usual solution is to this problem is to use a two-dye LIF approach, in which two fluorescent dyes are combines: one that is sensitive to the temperature, and one that is insensitive to temperature, i.e., to measure the local laser intensity (Sakakibara and Adrian 1999). However, this makes the whole optical configuration and experimental procedure very complicated. Instead, we apply a single-laser and single-dye LIF method using the pulsed Nd:YAG laser for both the LIF and PIV measurements. The pulse-to-pulse variation of the beam intensity and profile are accounted for in the data reduction procedure.

Figure 2a shows an example of an individual measurement of the fluorescence intensity; a detail of this result is shown in Figure 2b, which clearly shows that the fluorescence image contains striations. These are the result of several combined effects, such as the shawods cast by particles of the wall of the test section where the light sheet enters the test section, and refraction due to the local variation in fluid density (i.e., optical refractive index of the fluid). These striations complicate the accurate measurement of the temperature fluctuations, but can be removed by means of a two-dye LIF implementation (Sakakibara and Adrian 2004). Instead we use a simplified approach where we use an image processing approach by means of a simple spatial filter in order to reduce the effect of striations. Here we make use of the fact that our laser light sheet is collimated so that all light rays are parallel to the lines in the digital image, and suppress the DC components of the horizontal Fourier transforms over a specific wavenumber range. Figure 2c shows the result after appliciation of the spatial filter.

Experiments were carried out on a jet flow at a Reynolds number of 2×10^3. The jet fluid is cooled to a temperature 5° C before it enters the test section, which contains fluid (i.e., water) at room temperature (∼22° C). The jet fluid is extracted from the test section before the experiment, which ensures that both the jet fluid and the ambient fluid contain the same dye concentration and tracer particle concentration. Buoyancy effects in the cooled jet can be ignored for a distance from the nozzle z that is smaller than the Morton length scale ℓ_M defined as (Diez et al. 2003)

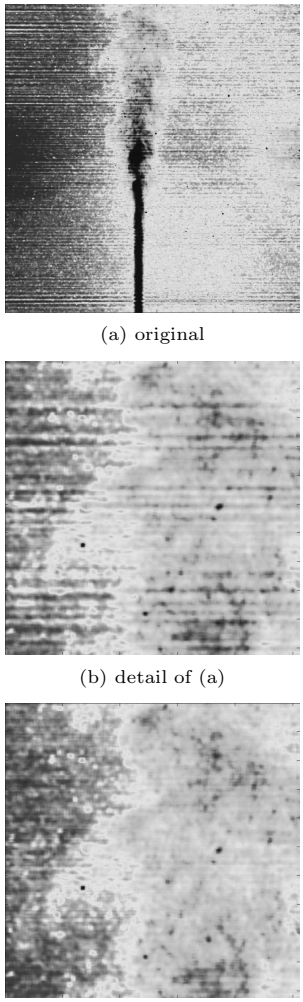

(a) original

(b) detail of (a)

(c) (b) after filtering

Figure 2: Example of instantaneous fluorescence image (in false color; red is high intensity, blue is low intensity).

$$\ell_M = \frac{M_0^{3/4}}{B_0^{1/2}}, \tag{1}$$

where M_0 is the momentum flux at the nozzle exit and B_0 the buoyancy flux at the nozzle exit, given by

$$M_0 = Q_0 U_0 \quad \text{and} \quad B_0 = Q_0 g(\Delta\rho/\rho), \tag{2}$$

where Q_0 is the volume flow rate at the nozzle, U_0 the mean velocity at the nozzle, g the gravitational acceleration, ρ the fluid density, and $\Delta\rho$ the fluid density variation due to the temperature difference. For the present experimental conditions we have $U_0 = 2$ m/s, $Q_0 = 1.5\times10^{-6}$ m^3/s, and $g = 10$ m/s^2. The density of water at 20° C and 5° C is 998.2 kg/m^3 and 1000 kg/m^3 respectively, so despite the large temperature difference, we have a relative density variation of $\Delta\rho/\rho \cong 1.8\times10^{-3}$ only. This is primarily due to the fact that for water the variation of density as a function of temperature vanishes at 4° C, which allows us to use fairly large temperature differences without unwanted large density differences and associated buoyancy effects. Substitution in (1) yields a Morton length scale of $\ell_M \cong 0.3$ m.

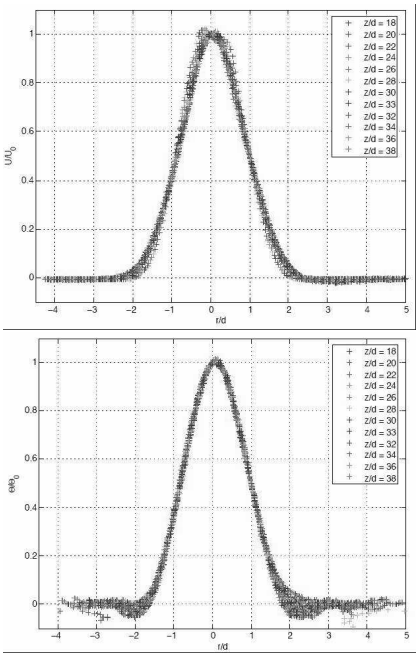

Figure 3: Normalized mean velocity profiles and mean temperature profiles at different locations from the jet nozzle.

This is equal to the length of the test section. Given that all our measurements are carried out at a distance z from the nozzle that smaller than ℓ_M, buoyancy effects can be neglected.

RESULTS

In total more than 10^3 simultaneous sets of LIF/PIV images were recorded. After processing we determined the conventional turbulence statistics, such as the mean centerline velocity U_c, mean centerline temperature difference Θ_c, and mean jet width b, all as a function of the downstream distance from the nozzle. The results of our measurements show the characteristics of a self-similar jet, i.e. the centerline velocity and mean temperature difference increase inversely proportional to the distance from the jet nozzle, whereas the jet half-width increases proportional to the distance from the nozzle. When the mean velocity and mean temperature difference are scaled with U_c and Θ_c respectively, and the radial coordinate is scaled with the jet half-width, then all profiles collapse on a single curve, as shown in Figure 3. This validates that the jet within our observation region is indeed self-similar. Similar profiles for the turbulent intensity of the axial and radial components of the velocity fluctuations and for the root-mean-square temperature fluctuations are shown in Figure 4. The Reynolds stress, and axial and radial turbulent temperature fluxes are shown in Figure 5. It is evident from Fig. 4 that the experimental data can only considered to be self-similar from about 34 nozzle diameters downstream. Also, the profile for the rms of the temperature fluctuations is not fully symmetric, and shows higher amplitudes on the side where the jet is illuminated. This indicates that the asymmetry may be due to self-absorption of the fluorescent dye.

In order to investigate the flow behavior at the interface of the turbulent/non-turbulent fluid motion, it is neccessary to detect the interface. In a previous study where only the

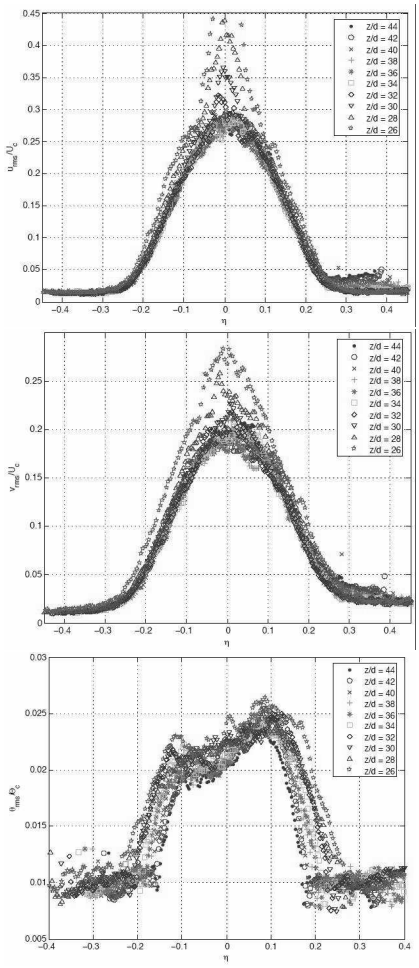

Figure 4: The turbulence intensity in the axial (left) and radial (middle) velocity components and the rms of the temperature fluctuations (right) as a function of the dimensionless coordinate $\eta = r/z$.

jet fluid contained a fluorescent dye, it was possible to detect the interface in a simple manner (Westerweel et al. 2005). In the present experiment this is no longer the case, and we have to revert to a more indirect method. We make use of the alternative detection methods proposed by Holzner et al. (2006). They propose to use either the magnitude of the estimated vorticity fluctuations or the magnitude of the velocity fluctuations to indicate the turbulent flow region.

We then proceed by taking flow statistics relative to the detected interface, as described by Westerweel et al. (2005). The results for the conditional mean temperature difference and conditionsl mean vorticity are shown in Figure 6. The conditional vorticity shows a very large jump at the interface, which essentially separates the irrotational and turbulent flow regions. The very steep gradient at the interface indicates that the interface detection method based on the turbulent kinetic energy is a reliable and robust alternative estimate. The vorticity profile even shows the small peak that is associated with the superlayer jump in the mean conditional axial velocity (Westerweel et al. 2005).

CONCLUSIONS

The present paper describes the experimental investigation of a cooled turbulent jet. The aim of the experiment is to investigate the flow characteristics near the

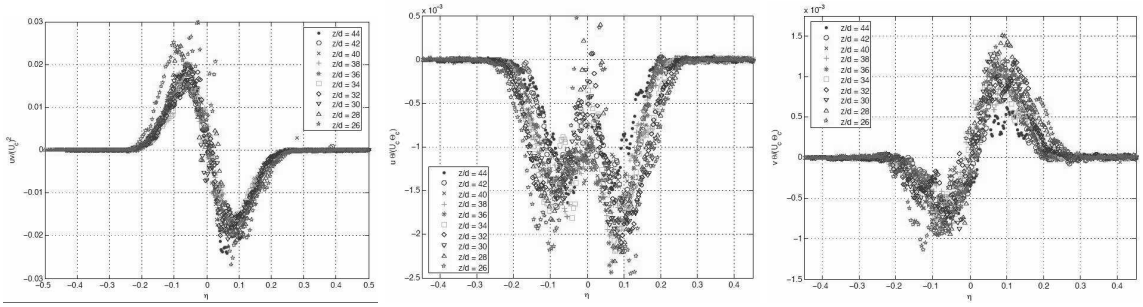

Figure 5: The Reynolds stress (left) and the axial (middle) and radial (right) turbulent heat fluxes as a function of the dimensionless coordinate $\eta = r/z$.

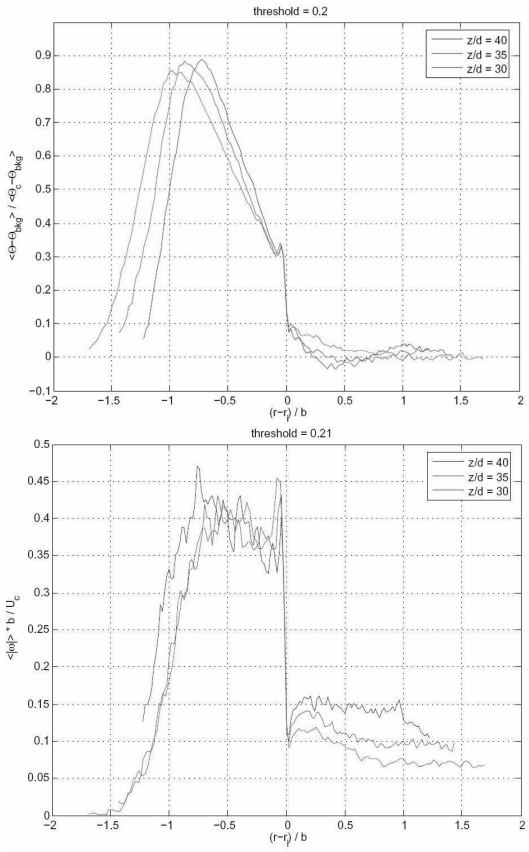

Figure 6: The conditional mean temperature (top) and the conditional mean vorticity (bottom) as a function of the distance from the interface.

turbulent/non-turbulent interface. A combined LIF/PIV method was used for the simultaneous measurement of the instantaneous velocity field and temperature field in a planar cross section through the jet centerline. The measurements are taken in a region where buoyancy effects can be neglected, and the jet in our experimental facility has the characteristics of a (neutrally buoyant) self-similar round jet. The detection of the turbulent/non-turbulent interface is based on the evaluation of the instantaneous magnitude of the kinetic energy fluctuation, as suggested by Holzner et al. (2006). Conditional averages of the axial velocity, temperature difference, and the vorticity relative to the detected turbulent/non-turbulent interface were computed. The large jump of vorticity that is observed validates the correct detection of the inteface. The conditional averages for the axial velocity and the temperature difference show the behavior that is expected for a laminar superlayer, i.e. a jump occurs at the interface. The jump in the velocity is of the same order of magnitude as reported previously (Westerweel et al. 2005), which was shown to be in agreement to the outward propagation velocity, or entrainment velocity, of the jet interface. The relative jump in the temperature is significantly larger than the relative jump in the velocity, yet it is significantly lower than the jump in the concentration, as reported by Westerweel et al. (2005). This is in agreement with a prediction that the magnitude of the jump is proportional to the turbulent transport coefficient, i.e., eddy viscosity for axial velocity, eddy thermal diffusivity for the temperature, and eddy mass diffusivity for the concentration; Further analysis of the present experimental data will be incorporated in a forthcoming paper.

*

References

Bisset, D. K., J. C. R. Hunt, and M. M. Rogers (2002). The turbulent/non-turbulent interface bounding a far wake. *J. Fluid Mech. 451*, 383–410.

Brown, G. L. and A. Roshko (1974). On density effects and large structure in turbulent mixing layers. *J. Fluid Mech. 64*, 775–816.

Corrsin, S. and A. L. Kistler (1955). Free-stream boundaries of turbulent flows. Technical Report 1244, NACA, Washington DC.

Diez, F. J., L. P. Bernal, and G. M. Faeth (2003). Round turbulent thermals, puffs, starting plumes and starting jets in uniform crossflow. *J. Heat Transf. 125*, 1046–1057.

Fukushima, C., L. Aanen, and J. Westerweel (2002). Investigation of the mixing process in an axisymmetric turbulent jet using PIV and LIF. In R. J. Adrian *et al.* (Ed.), *Laser Techniques for Fluid Mechanics*, pp. 339–356. Berlin: Springer.

Hinze, J. O. (1975). *Turbulence*. New York: McGraw-Hill.

Hishida, K. and J. Sakakibara (2000). Combined planar laser-induced fluorescence-particle image velocimetry technique for velocity and temperature fields. *Exp. Fluids 29*, S129–S140.

Holzner, M., A. Liberzon, M. Guala, A. Tsinober, and W. Kinzelbach (2006). Generalized detection of a turbulent front generated by an oscillating grid. *Exp. Fluids 41*, 711–719.

Hunt, J. C. R., N. D. Sandham, J. C. Vassilicos, B. E. Launder, P. A. Monkewitz, and G. F. Hewitt (2001).

Developments in turbulence research: A review based on the 1999 programme of the isaac newton institute, cambridge. *J. Fluid Mech. 436*, 353–391.

Mathew, J. and A. Basu (2002). Some characteristics of entrainment at a cylindrical turbulence boundary. *Phys. Fluids 14*, 2065–2072.

Sakakibara, J. and R. J. Adrian (1999). Whole field measurement of temperature in water using two-color laser induced fluorescence. *Exp. Fluids 26*, 7–15.

Sakakibara, J. and R. J. Adrian (2004). Measurement of temperature field a rayleigh-bénard convection using two-color laser-induced fluorescence. *Exp. Fluids 37*, 331–340.

Townsend, A. A. (1976). *The Structure of Turbulent Shear Flow* (2nd ed.). Cambridge University Press.

Tsinober, A. (2001). *An Informal Introduction to Turbulence*. Dordrecht: Kluwer.

Walker, D. A. (1987). A fluorescent technique for measurement of concentration in mixing liquids. *J. Phys. E Sci. Instrum. 20*, 217–224.

Westerweel, J., C. Fukushima, J. M. Pedersen, and J. C. R. Hunt (2005). Mechanics of the turbulent/nonturbulent interface of a jet. *Phys. Rev. Lett. 95*, 174501.